

Effects of Induction Heat Bending Process on Microstructure and Corrosion Properties of ASME SA312 Gr.TP304 Stainless Steel Pipes

Nam In Kim¹, Young Sik Kim^{1*}, Kyung Soo Kim², Hyun Young Chang²,
Heung Bae Park², and Gi Ho Sung³

¹Materials Research Center for Clean and Energy Technology, School of Materials Science and Engineering Materials, Andong National University, 1375 Gyeongdongro, Andong, Gyeongbuk, 760-749, Korea

²KEPCO Engineering & Construction Company, Power Engineering Research Institute, 8 Gumiro, Bundang, Seongnam, Gyeonggi, 463-870, Korea

³R&D Center, Sungil SIM, 1587-4 Songjung, Gangseo, Busan, 618-270 Korea

(Received January 08, 2015; Revised June 26, 2015; Accepted June 29, 2015)

The usage of bending products recently have increased since many industries such as automobile, aerospace, shipbuilding, and chemical plants need the application of pipings. Bending process is one of the inevitable steps to fabricate the facilities. Induction heat bending is composed of compressive bending process by local heating and cooling. This work focused on the effect of induction heat bending process on the properties of ASME SA312 Gr. TP304 stainless steel pipes. Tests were performed for base metal and bended area including extrados, intrados, crown up, and down parts. Microstructure was analyzed using an optical microscope and SEM. In order to determine intergranular corrosion resistance, Double Loop Electrochemical Potentiokinetic Reactivation (DL-EPR) test and ASTM A262 practice A and C tests were done. Every specimen revealed non-metallic inclusion free under the criteria of 1.5i of the standard and the induction heat bending process did not affect the non-metallic inclusion in the alloys. Also, all the bended specimens had finer grain size than ASTM grain size number 5 corresponding to the grain sizes of the base metal and thus the grain size of the pipe bended by induction heat bending process is acceptable. Hardness of transition start, bend, and transition end areas of ASME SA312 TP304 stainless steel was a little higher than that of base metal. Intergranular corrosion behavior was determined by ASTM A262 practice A and C and DL-EPR test, and respectively step structure, corrosion rate under 0.3 mm/y, and Degree of Sensitization (DOS) of 0.001 ~ 0.075 % were obtained. That is, the induction heat bending process didn't affect the intergranular corrosion behavior of ASME SA312 TP304 stainless steel.

Keywords : induction heat bending, 304 stainless steel, microstructure, intergranular corrosion

1. Introduction

Cooling system of the reactor in nuclear power plants are mostly made of austenitic stainless steel because of water chemistry. Austenitic stainless steels have good corrosion resistance and performance in the system but the steels may be sensitized by welding or improper heat treatment. In order to prevent the sensitization of austenitic stainless steels, the following remedies are recommended ASME SA312¹⁾; (a) solution heat treated in the range of 1,037.8 ~ 1,121.1 °C for 0.5 ~ 1 hour and then water quenched, (b) materials inspection program (especially ASTM A262²⁾etc.) applied, and (c) others – low carbon grade stainless steels or avoidance to the range of 426.7

~ 815.6 °C.

Recently, the application of bending products has been increased since the industries such as automobile, aerospace, ships, and plants greatly need the usage of pipes. For facility fabrication, bending process is one of key technologies for pipings. Induction heat bending process is composed of bending deformation by repeated local heat and cooling³⁾. Because of local heating and compressive strain, detrimental phases may be precipitated and microstructural change can be induced⁴⁾. This group reported the effect of induction heat bending process on the properties of ASME SA312 TP316 stainless steel⁵⁾. On the base of microstructural analysis, grain boundaries in bended extrados area were zagged by bending process, but there were no precipitates in grain and grain boundary and the intergranular corrosion rate was similar to that of base metal. However, pitting potentials of bended

* Corresponding author: yikim@anu.ac.kr

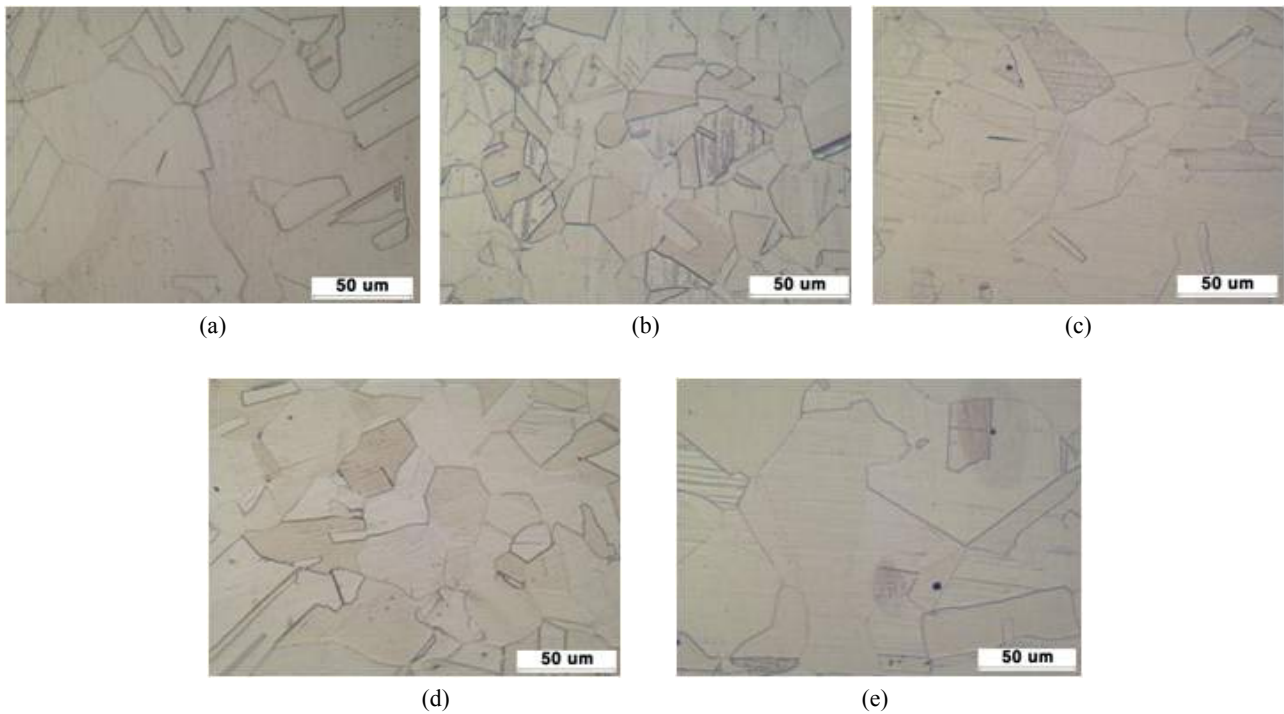


Fig. 2. Optical microstructure of internal surface of ASME SA312 TP304 stainless steel bent pipe (etchant: 90 ml HCl + 30 ml HNO₃ + 40 ml methanol) ; (a) base metal, (b) transition (start)-intrados, (c) transition (start)-extrados, (d) transition (start)-crown up, and (e) transition (start)-crown down.

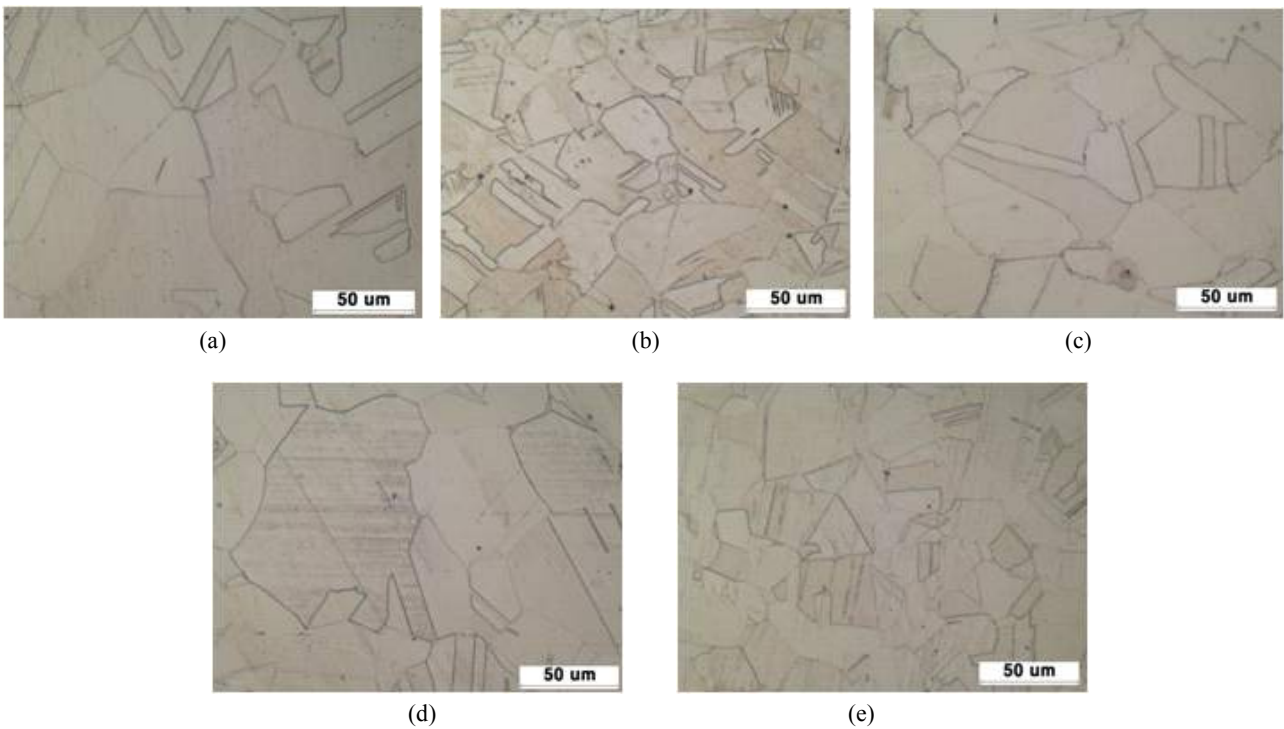


Fig. 3. Optical microstructure of internal surface of ASME SA312 TP304 stainless steel bent pipe (etchant: 90 ml HCl + 30 ml HNO₃ + 40 ml methanol) ; (a) base metal, (b) bend-intrados, (c) bend-extrados, (d) bend-crown up, and (e) bend-crown down.

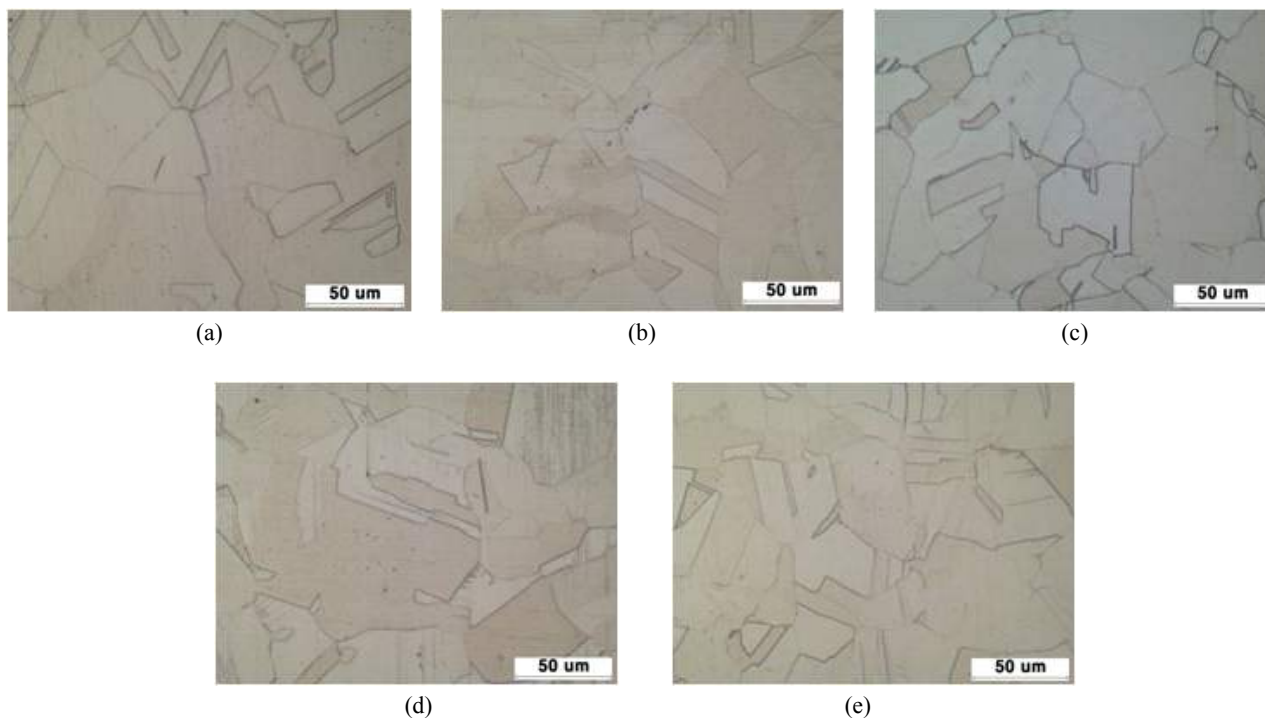


Fig. 4. Optical microstructure of internal surface of ASME SA312 TP304 stainless steel bent pipe (etchant: 90 ml HCl + 30 ml HNO₃ + 40 ml methanol); (a) base metal, (b) transition (end)-intrados, (c) transition (end)-extrados, (d) transition (end)-crown up, and (e) transition (end)-crown down.

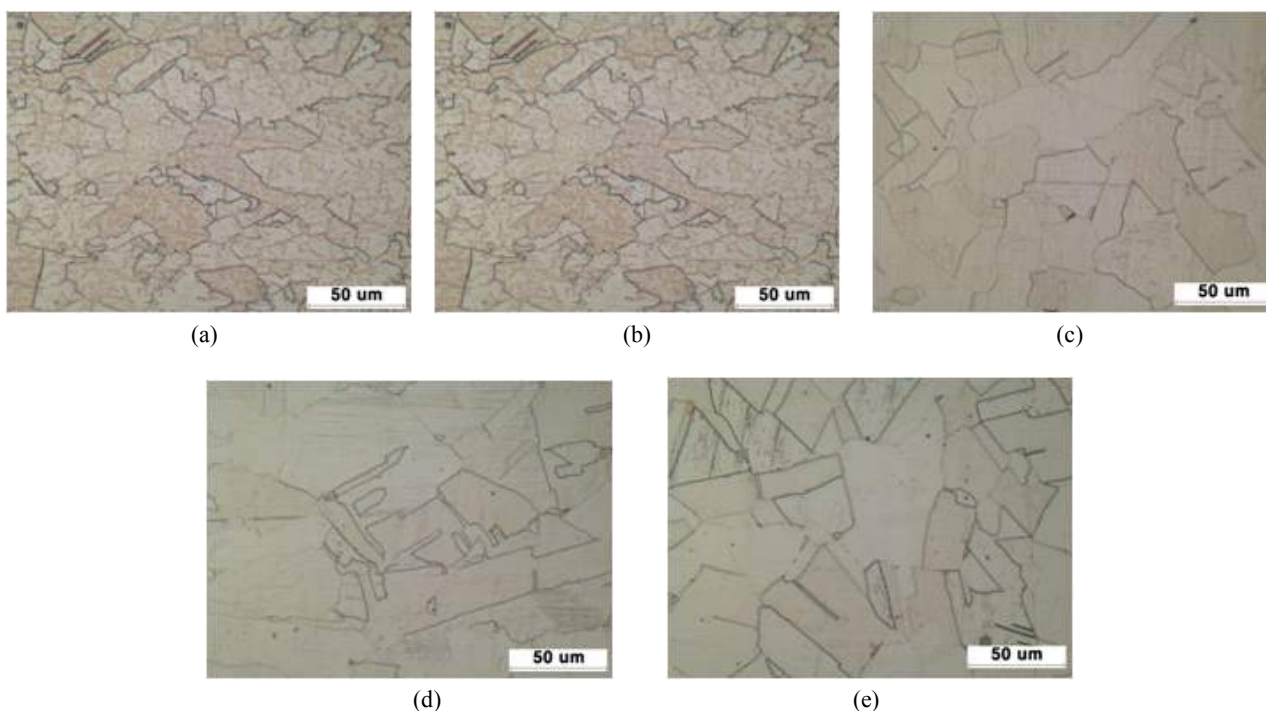


Fig. 5. Optical microstructure of cross section of ASME SA312 TP304 stainless steel bent pipe (etchant: 90 ml HCl + 30 ml HNO₃ + 40 ml methanol); (a) base metal, (b) bend-intrados, (c) bend-extrados, (d) bend-crown up, and (e) bend-crown down.

does not affect the non-metallic inclusion in the alloys.

Fig. 2 shows the optical microstructure of internal surface of transition start areas of ASME SA312 TP304 stainless steel bent pipe (etchant: 90 ml HCl + 30 ml HNO₃ + 40 ml methanol). Regardless of base metal and bended areas, lots of twins were observed and the grain size was different with each other. The extrados area can be usually tensile-stressed during bending process, but this induction heat bending process is performing under the compressive force. Therefore, every specimen showed typical austenitic microstructure such as twin and each grain size was a little different but almost similar microstructure.

Fig. 3 reveals the optical microstructure of internal surface of bended areas of ASME SA312 TP304 stainless steel bent pipe (etchant: 90 ml HCl + 30 ml HNO₃ + 40 ml methanol). As like that of transition start area shown in Fig. 2, regardless of base metal and bended areas, lots of twins were observed and the grain size was different with each other. This is also due to the compressive force during bending process.

Fig. 4 represents the optical microstructure of internal surface of transition end areas of ASME SA312 TP304 stainless steel bent pipe (etchant: 90 ml HCl + 30 ml HNO₃ + 40 ml methanol). As like those of transition start and bended areas shown in Fig. 2 and Fig. 3, regardless of base metal and bended areas, lots of twins were observed and the grain size was different with each other. This is also due to the compressive force during bending process.

Fig. 5 shows the optical microstructure of cross section of ASME SA312 TP304 stainless steel bent pipe (etchant: 90ml HCl + 30ml HNO₃ + 40ml methanol). The specimens

including base metal and bended areas showed typical austenitic microstructure such as twin and each grain size was a little different but almost similar microstructure. However, optical microstructure of the cross section was zagged than that of surface microstructure.

Fig. 6 summarizes ASTM grain size of base metal, transition start, bend, transition end areas of ASME SA312 TP304 stainless steel determined by ASTM E111¹⁰⁾. Every specimen showed finer grain size than ASTM grain size number 5 and thus its grain size is acceptable even induction heat bending process.

Fig. 7 shows the surface hardness of base metal, transition start, bend, transition end areas of ASME SA312 TP304 stainless steel. Hardness was measured by Rockwell hardness tester, B scale. Hardness of base metal was HRB 76.2. But hardness of bend areas has a rage of HRB 83~88 and hardness of transition start areas showed HRB 83~87 and hardness of transition end areas was HRB 83~88. Surface hardness was increased by induction heat bending process, because bending process was performing under thermomechanical condition. Especially, the hardness of intrados and transition end areas was relatively high. This behavior seems to be related to bending and thermal stress.

Degree of sensitization of base metal, transition start, bend, transition end areas of ASME SA312 TP304 stainless steel was determined by ASTM A262 practice A²⁾. Every area showed ‘step structure’ and thus was all acceptable. Another method by DL-EPR⁵⁾ was performed. Test condition was 30 °C, 0.5M H₂SO₄ + 0.01M KSCN and its scan rate was 1.67 mV/sec. The result of DL-EPR test was shown in Fig. 8. Every specimen shows the active peak by the forward polarization and their values

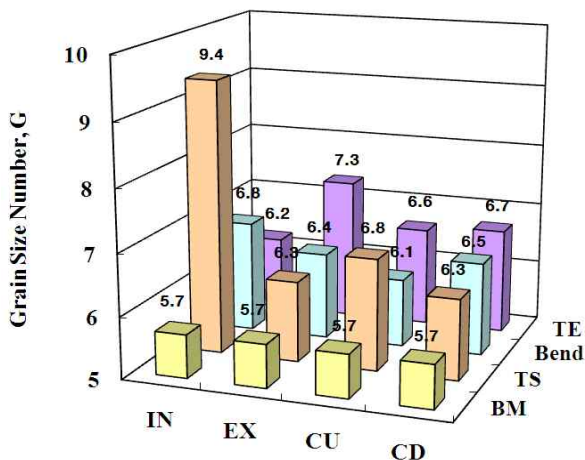


Fig. 6. ASTM grain size of base metal, transition start, bend, and transition end areas of ASME SA312 TP304 stainless steel.

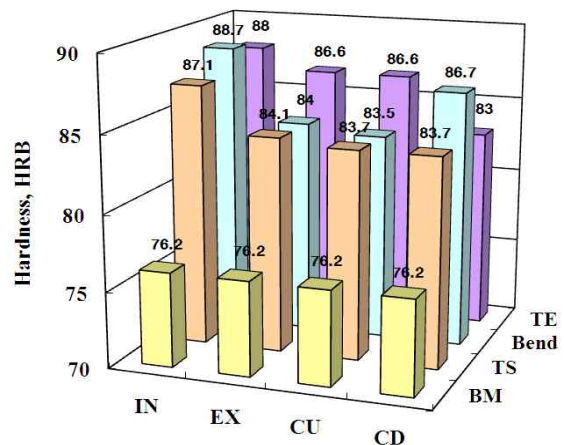


Fig. 7. Surface hardness of base metal, transition start, bend, transition end areas of ASME SA312 TP304 stainless steel.

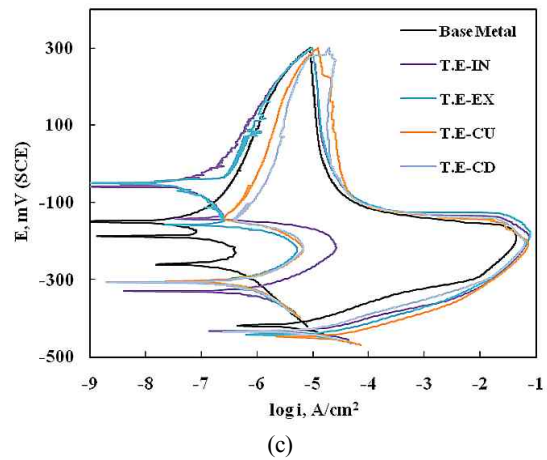
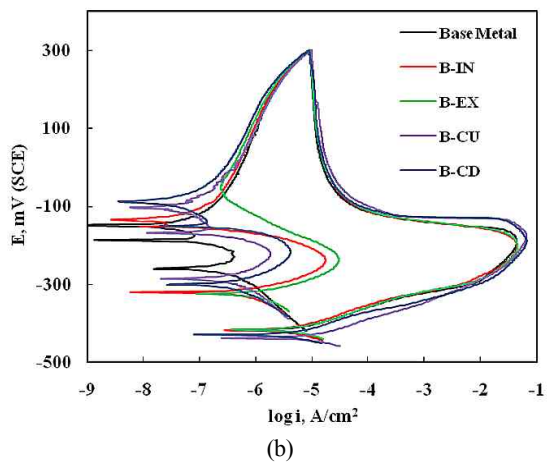
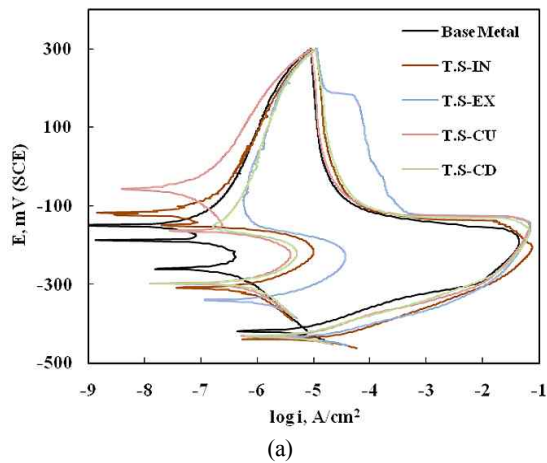


Fig. 8. DL-EPR test of ASME SA312 TP304 stainless steel bent pipe; (a) transition start, (b) bend, and (c) transition end.

were similar each other regardless of transition start, bend, and transition end areas. Also, every specimen showed very small reactivation peaks by the reverse polarization and thus the ratios of DOS were calculated as 0.001 ~ 0.075 % as shown in Table 2. This is co-

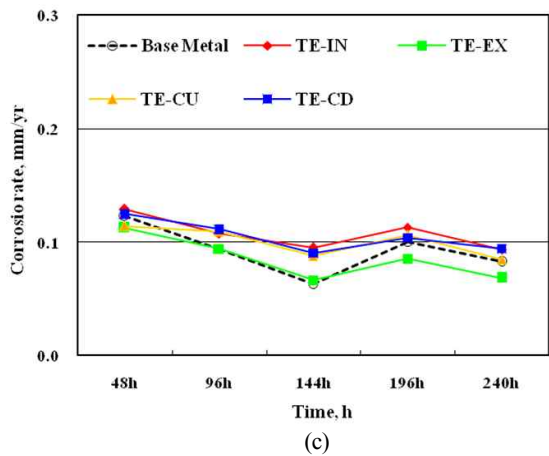
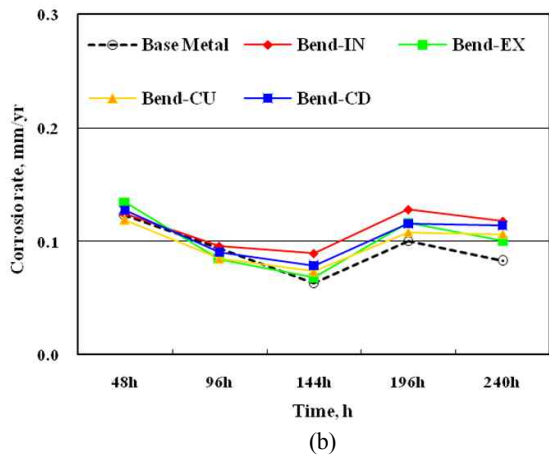
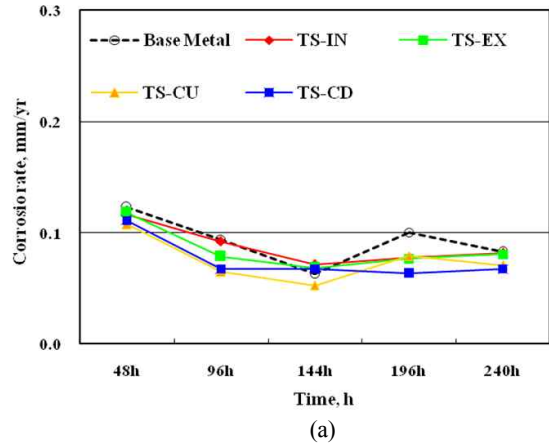


Fig. 9. Effect of test periods on the corrosion rate by ASTM A262 practice C of (a) transition start, (b) bend, and (c) transition end of ASME SA312 TP304 stainless steel.

incident with the result of ASTM A262 practice A. Fig. 9 shows the effect of test periods on the corrosion rate by ASTM A262 practice C of (a) transition start, (b) bend, and (c) transition end of ASME SA312 TP304 stainless steel. Regardless of bend areas, small inter-

Table 2. DOS by DL-EPR test in 0.5M H₂SO₄ + 0.01M KSCN on base metal, transition start, bend, and transition end areas of ASME SA312 TP304 stainless steel

Areas	Log I _a (A/cm ²)	Log I _r (A/cm ²)	DOS (%)
Base metal	-1.446	-6.408	0.001
Transition start – Intrados	-1.252	-4.435	0.065
Transition start – extrados	-1.224	-4.435	0.061
Transition start – Crown up	-1.220	-5.404	0.006
Transition start – Crown down	-1.278	-5.293	0.009
Bend – Intrados	-1.447	-4.763	0.048
Bend – extrados	-1.401	-4.524	0.075
Bend – Crown up	-1.297	-5.749	0.003
Bend – Crown down	-1.239	-5.381	0.007
Transition end – Intrados	-1.196	-4.591	0.040
Transition end – extrados	-1.185	-5.284	0.007
Transition end – Crown up	-1.238	-5.176	0.011
Transition end – Crown down	-1.272	-5.179	0.012

granular corrosion rates were determined. Intergranular corrosion rate of every specimen was under 0.3 mm/y and thus was acceptable. This implies that induction heat bending process didn't affect the intergranular corrosion behavior of ASME SA312 TP304 stainless steel.

4. Conclusions

Every specimen revealed non-metallic inclusion free under the criteria of 1.5i of the standard and induction heat bending process does not affect the non-metallic inclusion in the alloys. Also, every specimen showed finer grain size than ASTM grain size number 5 and thus the grain size of the bened pipe is acceptable. Hardness of transition start, bend, and transition end areas of ASME SA312 TP304 stainless steel was a little higher than that of base metal. Intergranular corrosion behavior was determined by ASTM A262 practice A and C and DL-EPR test and respectively step structure, corrosion rate under 0.3 mm/y, and DOS of 0.001 ~ 0.075 % were obtained. That is, induction heat bending process didn't affect the intergranular corrosion behavior of ASME SA312 TP304 stainless steel.

Acknowledgments

Research for this paper was supported by Sungil SIM Company funded from the Korea Institute for the Advancement of Technology. Authors wish to thank both organizations.

References

1. ASME II, Part A Ferrous Materials Specifications (Beginning to SA-450) (2011).
2. ASTM A262, *Standard practices for detecting susceptibility to intergranular attack in austenitic stainless steels* (2002).
3. H. Blume, W. E. Speth, and K. Bredenbruch, *Energy Dev.*, **12**, 9 (1983).
4. W. D. Callister, Jr., *Materials Science and Engineering, An Introduction*, John Wiley & Sons, Inc. (2003).
5. M. C. Shin and Y. S. Kim, *Corros. Sci. Tech.*, **13**, 88 (2014).
6. H. C. Choe and K. T. Moon, *J. Corros. Sci. Soc. of Kor.*, **21**, 239 (1992).
7. Y. H. Kim, D. Y. Ryoo and Y. D. Lee, *J. Corros. Sci. Soc. of Kor.*, **21**, 111 (1992).
8. ASTM G108, *Standard test method for electrochemical reactivation (EPR) for detecting sensitization of AISI type 30 and 304L stainless steels* (1994).
9. ISO 4697, *Steel-Determination of content of non-metallic inclusions micrographic method using standard diagrams* (2013).
10. ASTM E112, *Standard test method for determining average grain size* (2004).